NASA TN D-1265

NASA TN D-1265

TECHNICAL NOTE

D-1265

DETERMINATION OF THE CREEP DEFLECTION AND LIFETIME OF ALUMINUM-ALLOY MULTIWEB BOX BEAMS SUBJECTED TO VARIED LOADS AT CONSTANT TEMPERATURE

By Avraham Berkovits

Langley Research Center
Langley Station, Hampton, Va.

NATIONAL AERONAUTICS AND SPACE ADMINISTRATION
WASHINGTON
June 1962

NATIONAL AERONAUTICS AND SPACE ADMINISTRATION

TECHNICAL NOTE D-1265

DETERMINATION OF THE CREEP DEFLECTION AND LIFETIME OF ALUMINUM-ALLOY MULTIWEB BOX BEAMS SUBJECTED TO VARIED LOADS AT CONSTANT TEMPERATURE

By Avraham Berkovits

SUMMARY

A method was developed for computing the deflection and lifetime of multiweb box beams subjected to creep under varied loads at constant temperatures. The method of analysis is based on the life-fraction rule and materials creep data obtained from constant-load and constant-temperature tensile creep tests. Calculated deflection and lifetime results are compared with corresponding test data from multiweb box beams fabricated from 2024-T3 aluminum-alloy sheet and tested at 400° F under cyclic creep loads. An equivalent-stress concept is utilized in a portion of this study to reduce the varied-load creep problem to creep under constant stress.

INTRODUCTION

Structural components of vehicles which are subject to aerodynamic heating may undergo creep deformations which are of concern in structural design. Considerable research has been carried out on structural creep under constant load and constant temperature. Semiempirical methods for determining the creep lifetime of components such as beams, panels, and cylinders are presented in references 1 to 4. An analysis for estimating the deflection of a beam under an essentially constant creep load is presented in reference 5.

Recent interest in the field of creep has focused on problems involving varying load and temperature conditions, because structural components are generally subjected to unsteady loads and temperatures during service. In reference 6, a study is made of three hypotheses for predicting material creep behavior under varied loads at constant temperature. The study of reference 6 is extended to structural components in the present investigation. Relationships are developed for estimating creep deflection and lifetime of beams under varied loads by

use of the life-fraction rule. The method utilizes materials creep data obtained at constant load and constant temperature. The calculated results are compared with data obtained from varied-load creep tests performed on multiweb box beams fabricated of 2024-T3 aluminum alloy.

SYMBOLS

A, k, σ_o	empirical creep constants, see equation (1)
a	cross-sectional area of beam, sq in.
b	bay width, in. (fig. 1(c))
E	Young's modulus, ksi
h	beam height between midplanes of beam cover sheets, in. (fig. 1(c))
K	buckling coefficient
l_1	length of beam between supports, in. (fig. 1(a))
l_2	length of beam between support and load point, in. (fig. 1(a))
l	one-third of beam length when $l_1 = l_2$, in.
M	bending moment, in-kips
t	cover-sheet thickness, in. (fig. 1(c))
x,y	coordinates, in. (fig. 1(b))
ϵ	strain
μ	Poisson's ratio
σ	stress, ksi
τ	time, hr

Subscripts:

c	compression
cr	critical (buckling)

cy	compressive yield
eq	equivalent
e	edge
f	failure
i,j,n	integers
mid	midpoint
s	secant
t	tension
tip	tip
ult	ultimate

DEVELOPMENT OF DEFLECTION AND LIFETIME RELATIONSHIPS

Relationships for determining the deflection of a beam subjected to varied-load creep at constant temperature were developed in the following manner. The stresses occurring in the beam were determined from the externally applied load by use of static equilibrium relationships in conjunction with a material creep law. These calculations involved an iterative procedure which utilized the IBM 650 digital computer. Integration of the classical relationship between beam curvature and strain yielded expressions for beam deflection in terms of the materials creep law. The life-fraction rule was applied to the beam deflection equations to obtain deflection under varied-load creep.

Static strength and plate-buckling relations were used in conjunction with the materials creep law and the equivalent-stress concept to predict lifetime, local buckling, and the deflection of a buckled beam during creep.

Materials Creep Law for Constant and Varied Loads

The expression used to describe strain of the beam material under constant-load creep at constant temperature was taken to be

$$\epsilon = \frac{\sigma}{E} + A\tau^{k} \sinh \frac{\sigma}{\sigma_o} \qquad (1)$$

Equation (1) was selected because it describes material behavior in the primary creep region over a wide range of stresses. This form of materials creep law was used in reference 6 and in other studies. Both tensile and compressive strain were calculated from equation (1).

In selecting a suitable relationship for the creep of the material in a built-up structure, it is important to consider the magnitude of strains expected in the structure. Observation of structures such as multiweb box beams indicates that initiation of collapse occurs at extreme fiber strains generally less than 0.005 (ref. 4). In the region of such strains consideration of primary creep as given in equation (1) is usually sufficient.

L
1
4
6
4

Equation (1) was modified for the varied-load creep problem with the aid of the life-fraction rule. In accordance with the life-fraction rule, the creep behavior of a material depends on the fraction of lifetime which has been consumed. The rule can be illustrated by consideration of a creep test during which a material is subjected for a time τ_1 to an initial stress σ_1, with a corresponding lifetime $\tau_{f,1}$. The stress is then changed to σ_2 with a lifetime $\tau_{f,2}$. The creep behavior of the material during time τ_1 is described by the creep curve for σ_1; subsequent to the stress change, the creep behavior is described by the creep curve for σ_2, beginning at time

$$\tau = \frac{\tau_1}{\tau_{f,1}} \tau_{f,2} \tag{2}$$

The life-fraction rule was selected in the present study for: (a) ease of mathematical application in the case of an unbuckled beam and (b) the equivalent stress developed from the rule and discussed subsequently. Application of the life-fraction rule to the materials creep law given by equation (1) is described in detail in reference 6. The strain equation developed in reference 6 for varied-load creep will be applied in the discussion of beam behavior under varied loads.

Static Equilibrium

The stresses occurring in a beam during creep must be determined from the external bending moment before beam deflection can be computed from the creep law given by equation (1). Internal stresses associated

with an applied moment M were determined by the solution of the thrust and moment equilibrium equations:

$$\left.\begin{aligned} \int \sigma \, da &= 0 \\ \int \sigma y \, da - M &= 0 \end{aligned}\right\} \tag{3}$$

For most built-up structures, equations (3) must be evaluated by numerical integration. In the present study the cross section of the box beams was divided through the depth into eleven elemental areas, the two outer elements consisting of the beam covers. The iterative procedure involved in evaluating equations (3) was performed with the use of the IBM 650 digital computer. In the calculations it was assumed that beam cross sections remain plane during creep, so that the strain varied linearly through the depth of the beam and the stresses could be determined from the materials creep law.

Beam Deflection

The form of the deflection relationships was determined by successive integration of the classical relationship between beam curvature and the strain in the compression and tension covers, and by substitution for the strain from the materials creep law (eq. (1)). The curvature is given by

$$\frac{d^2y}{dx^2} = \frac{1}{h}(\epsilon_t - \epsilon_c) \tag{4}$$

where ϵ_t and ϵ_c are the strains in the midplanes of the tension and compression covers, respectively, and h is the depth of the beam. Throughout the present study, tensile stress and strain are positive and compressive stress and strain are negative.

When the materials creep law is substituted into equation (4) the integration of the equation involves numerical procedures in many cases. In the present investigation, however, the loading and boundary conditions were such as to permit direct integration of equation (4). The multiweb box beam studied in this investigation was simply supported at two points equidistant from the midpoint and was loaded at each end (fig. 1(a)). In the analysis the beam was treated in two parts as shown in figure 1(b): the region between the supports, hereafter referred to as the inboard region, and the region between the support and the load, hereafter called the outboard region.

Boundary conditions for the inboard region are zero deflection at the supports. For the outboard region the boundary conditions at the support are zero deflection and outboard slope equal to inboard slope.

Deflection relations for a beam loaded as in figure 1 and subject to creep under varied bending loads at constant temperature are derived in the appendix. For the case in which $l_1 = l_2 = l$ the deflection at the midpoint and at the tip of the beam after application of i loads at constant temperature is obtained from the appendix as

$$y_{mid} = -\frac{l^2}{8h}\left\{\frac{\sigma_{t,i} - \sigma_{c,i}}{E} + A\left[\left(\sum_{n=1}^{n=i} \Delta\tau_n \sinh^{1/k} \frac{\sigma_{t,n}}{\sigma_o}\right)^k - \left(\sum_{n=1}^{n=i} \Delta\tau_n \sinh^{1/k} \frac{\sigma_{c,n}}{\sigma_o}\right)^k\right]\right\} \tag{5}$$

$$y_{tip} = \frac{l^2}{h}\left(\frac{5}{6}\frac{\sigma_{t,i} - \sigma_{c,i}}{E} + \frac{A}{2}\left[\left(\sum_{n=1}^{n=i} \Delta\tau_n \sinh^{1/k} \frac{\sigma_{t,n}}{\sigma_o}\right)^k - \left(\sum_{n=1}^{n=i} \Delta\tau_n \sinh^{1/k} \frac{\sigma_{c,n}}{\sigma_o}\right)^k\right] + A\left\{\sum_{n=1}^{n=i} \Delta\tau_n\left[\frac{\sigma_o}{\sigma_{t,n}} \cosh \frac{\sigma_{t,n}}{\sigma_o} - \left(\frac{\sigma_o}{\sigma_{t,n}}\right)^2 \sinh \frac{\sigma_{t,n}}{\sigma_o}\right]^{1/k}\right\}^k - A\left\{\sum_{n=1}^{n=i} \Delta\tau_n\left[\frac{\sigma_o}{\sigma_{c,n}} \cosh \frac{\sigma_{c,n}}{\sigma_o} - \left(\frac{\sigma_o}{\sigma_{c,n}}\right)^2 \sinh \frac{\sigma_{c,n}}{\sigma_o}\right]^{1/k}\right\}^k\right) \tag{6}$$

where σ_t and σ_c are the stresses in the inboard region of the tension and compression covers, respectively, $\Delta\tau_n = \tau_n - \tau_{n-1}$, and $\tau_0 = 0$. These relations are applied directly in the section entitled "Results and Discussion." In the derivation of equation (6), considerable simplification was achieved by applying the life-fraction rule to the deflection components and by assuming that the stress in the cover plates varied linearly from a maximum at the support to zero at the tip. Although this assumption was violated in the immediate vicinity of the support for some loads, the magnitude of the deflections calculated on the basis of this assumption was not expected to be appreciably different from results of a more rigorous analysis that would have taken the nonlinear stress distribution into account.

Postbuckling Deflection

The preceding deflection relationships apply to beams in which the strain in the compression cover is given directly by the materials creep law; that is, beams that do not undergo local out-of-plane buckling during creep. The approximate deflection of beams which exhibit local buckling prior to collapse was obtained by adaptation of a plate load-shortening equation for use with the materials creep law in the form of isochronous stress-strain curves, and by introduction of an equivalent stress. Use of isochronous stress-strain curves in creep problems is discussed in reference 7. This procedure reduced the varied-load problem to an equivalent soluble constant-load case.

The relationship between the average stress in a buckled plate and the average strain can be determined from the relation given in reference 8:

$$\sqrt{\frac{\epsilon_c}{\epsilon_{cr}}} = \frac{\sigma_e}{\sigma_c} \tag{7}$$

Equation (7) was used in conjunction with isochronous stress-strain curves calculated from equation (1). In equation (7), σ_c is the stress on the isochronous load-shortening curve for given strain ϵ_c, σ_e is the corresponding stress in equation (1), and the buckling strain ϵ_{cr} is assumed to be independent of time and is determined by the relation

$$\epsilon_{cr} = \frac{K\pi^2}{12\left(1 - \mu^2\right)}\left(\frac{t}{b}\right)^2 \tag{8}$$

where K is the buckling coefficient, μ is Poisson's ratio, and t/b is the thickness-width ratio of the compression cover plate (fig. 1(c)). It should be pointed out that the application of equation (7) is limited to cases in which ϵ_{cr} is of the magnitude usually associated with the elastic region of the material. Use of isochronous load-shortening curves to calculate the deflection of a buckled beam subjected to constant-load creep is described in the appendix.

Deflection of a buckled beam under varied-load creep was determined by use of an equivalent stress. The equivalent stress is defined in reference 6 as that stress which when applied continuously will produce failure at the same time as the varied stress condition. A relation for the equivalent stress is derived from the life-fraction rule in reference 6 for the case in which a varied-load sequence is repeated several times. The relation takes the form

L 1 4 6 4

$$\sinh \frac{\sigma_{eq}}{\sigma_o} = \left(\frac{\sum_{n=1}^{n=j} \Delta\tau_n \sinh^{1/k} \frac{\sigma_n}{\sigma_o}}{\sum_{n=1}^{n=j} \Delta\tau_n} \right)^k \tag{9}$$

where σ_{eq} is the equivalent stress and j is the number of loads per cycle. Although equation (9) was derived for a flat sheet it is assumed that σ_{eq} for a buckled sheet is the same as for a sheet which remains flat and is subjected to the same stress cycle. When the equivalent stresses for the compression and tension covers have been ascertained from equation (9) the deflection of the beam can be determined as for a beam under constant creep load as described in the appendix.

Lifetime

Failure of the box-beam type of structure usually occurs in the compression cover. For given lifetimes, stress in the compression cover of the beam was computed from a plate strength and lifetime relation, of the form given in reference 3:

$$\sigma_f = 1.6\sqrt{E_s \sigma_{cy}} \frac{t}{b} \tag{10}$$

In equation (10) E_s is the secant modulus associated with failure stress σ_f, and σ_{cy} is the 0.002-offset stress for the isochronous stress-strain curve corresponding to a given lifetime. For beams subjected to varied loads, the creep-failure conditions were determined by reducing the varied-load problem to the equivalent constant-load problem by use of the equivalent stress for the compression cover.

EXPERIMENTAL PROGRAM

Test Specimens and Equipment

Two multiweb box-beam designs were investigated. Beams designated A had a nominal b/t value of 25 in the compression cover, so that the buckling and failure stresses would be in the plastic range of the material. The tension cover in this design was heavier than the compression cover to insure compression failures. Beams designated B had a nominal b/t value of 40, so that elastic buckling would occur prior to failure.

Tests were conducted on 19 beams fabricated from 2024-T3 aluminum-alloy sheet. The beams were about 96 inches long, simply supported at points 15.5 inches on either side of the midpoint (fig. 1(a)), and were loaded at the tips with the center of load acting 1.5 inches from each end. The beam height was about 3.5 inches and the width was approximately 10 inches, comprising three equal cells as shown in figure 1(c). Detailed dimensions of the beams are given in table I. The formed channel webs were riveted to the cover sheets and were reinforced against shear loads at the load and reaction points by the use of angle sections (fig. 2).

Varied loads were applied to the beams by means of a hydraulic cylinder as shown in figure 2, and constant loads were applied with deadweights supported in weight cages as shown in figure 3. Operation of the load programing equipment with which step loads were applied during the varied-load tests is discussed in detail in reference 6. Applied loads were measured with load cells mounted in the two loading columns. Deflections were measured at various points along the beams with the aid of deflectometers. Each deflectometer consisted of a small cantilever (fig. 2) on which wire resistance strain gages were mounted. The free end of the cantilever was attached to the beam specimen by a vertical steel wire. Time histories of the applied loads and beam deflections were recorded.

The beams were tested in an automatically controlled furnace. Variations in the furnace air temperature during any test were not greater

than ±3° F, and the temperatures at various points on the beams as well as in the furnace atmosphere were monitored by use of a twelve-channel temperature recorder.

Test Program

With one exception, all tests were performed at a temperature of 400° F, and in every case the load was applied after the beam had been exposed to the test temperature for 1/2 hour. The exposure time allowed the specimen and extensometer wires to reach equilibrium temperature before data zeros were taken. Creep tests were generally limited to a duration of 35 hours, because frequent monitoring of the load programer was necessary and overnight interruption of tests was required. Test conditions are given in table II.

Beams A1, B1, and B2 underwent static strength tests; beams A2, B3, and B4 were tested in creep under constant load and temperature. These preliminary tests were conducted in order to obtain data for use as reference or base values for the beams tested under varied loads.

Varied-load tests were conducted at constant temperature on 13 specimens. The load spectrum represented by the dashed-line curve in figure 4 was simulated by step loads which were applied in repeated sequences. The dashed-line curve was derived from the load history given for transport airplanes in reference 2. Note that in figure 4 the logarithmic scale of the abscissa is changed to a linear scale at 1 percent of time above load.

Loads such as given by curve A in figure 4 were applied to eight beams (A3 to A7 and B5 to B7) which were tested to failure in varied-load creep tests. In these tests each load cycle consisted of three load levels, and the duration of each cycle was 26 minutes. The low load in each cycle was applied for 20 minutes, the intermediate load for 4 minutes, and the high load for the remaining 2 minutes. Four of the varied-load creep tests were conducted with the loads in ascending sequence as described, and four were performed with the loads in descending sequence to study the effect of reversing the order of loading. The loads applied during the varied-load creep tests were high, as shown in curve A of figure 4, so that failures occurred in less than 35 hours. However, it was expected that results of the present tests would provide adequate comparison with results calculated from theory.

The five remaining beams were subjected to cyclic-load histories which approximated the loading represented by the dashed-line curve of figure 4 more closely than did the load histories applied during preceding tests. Load histories described by curves B and C in figure 4

were applied to determine whether significant creep would occur in 20 hours under simulated airplane loads. The lowest load in each 30-minute cycle was applied for 24.5 minutes, followed by increasingly higher loads, up to a maximum load of $\frac{2}{3} M_{ult}$. The maximum load was applied for 0.1 minute during each cycle; 0.1 minute is the minimum time-at-load obtainable with the load programer used. Each beam was subjected to 40 cycles of load, and a static-strength test was then performed on the beam at test temperature. One of the beams (A10) was subjected to load history B at 500° F, to obtain an indication of the influence of temperature on the test results.

RESULTS AND DISCUSSION

Creep deflection results and lifetime and strength results for the multiweb box beams are presented and discussed in this section. Calculated results are obtained by use of the following material creep constants:

$$E = 9.4 \times 10^3 \text{ ksi}$$

$$A = 6.8 \times 10^{-5}$$

$$k = 0.5$$

$$\sigma_o = 9.3$$

The material creep constants were obtained in tension in reference 6 from constant-load creep data for 2024-T3 aluminum-alloy sheet at 400° F, and are used for both tension and compression in the present calculations.

Deflection

Calculated deflection results are compared with experimental data obtained from the beams during constant-load and cyclic-load creep tests in figures 5 and 6, respectively. Comparisons are made for the magnitude of the midpoint and tip deflections for each beam.

Constant load.- Deflection data from constant-load creep tests of box beams are plotted against time in figure 5. The experimental curves end at the failure time of the test beams, and the theoretical (dashed) curves terminate at the calculated failure time. Although the magnitude of observed deflections compares well with calculated values, correlation between experiment and theory on the basis of time is not as

satisfactory. Results obtained from beams B3 and B4 indicate that the creep behavior of these lighter weight beams (b/t = 40) was highly sensitive to the value of the applied load.

Varied loads.- Results obtained from cyclic-load creep tests of box beams are presented in figure 6. Experimental deflections are indicated by the shaded areas which define the bounds of the data. The deflection during the first cycle is shown in greater detail than subsequent deflections. The dashed curves, which apply to beams A, were calculated from equations (5) and (6). The upper and lower bounds correspond to the highest and lowest load level applied in each load cycle, respectively. The calculated curves in figure 6 terminate at the calculated lifetime. Beams B underwent local buckling during the early part of the creep tests; the equivalent-stress method was therefore used to calculate deflections of these beams. The solid-line curves in figure 6 represent average creep deflection for the beams, calculated by introducing the equivalent stresses into the constant-load creep relationships.

L 1 4 6 4

It may be seen from figure 6 that the greater part of the test data obtained from beams A falls within the bounds predicted. The beam deflections computed by using the equivalent-stress concept approximated the data satisfactorily, except in the case of beam B5 which failed before the end of the second load cycle. Results show that the effect of the loading sequence within the cycle was negligible, and little evidence of scatter in duplicate tests was found. The agreement between calculated and experimental deflections achieved for beams loaded as in figure 1 indicates that the deflection of a beam under more complicated loadings could be calculated fairly accurately by numerical integration of equation (4) and the use of an appropriate creep law for the strains. (It is of interest that deflections predicted by the time-hardening and strain-hardening hypotheses discussed in reference 6 are within 3 percent of the life-fraction-rule results reported herein.)

No measurable creep deflection occurred in 20 hours during the tests in which the beams were subjected to load histories B and C of figure 4, either at 400° F or at 500° F. The strength of these beams after 20 hours under load is discussed in the following section.

Beam Failure

All beams tested failed in the inboard compression cover, regardless of the type of test performed. Two types of failure were observed. Beam A failed suddenly in the mode illustrated in figure 7(a) and showed no evidence of buckling prior to collapse. In beams B, local buckles (fig. 7(b)) were produced immediately by the applied load or appeared during the early part of creep tests. The depth of these buckles

increased during the tests until collapse occurred and a V-shaped buckle was formed across the specimen. The V-shaped buckle appearing at the failure points in figure 7 is more severe than at the instant of collapse, since the loading equipment did not release the load instantaneously when failure occurred. In general, the beams failed when the creep strain in the compression cover reached a value of approximately 0.0025, in agreement with conclusions drawn in reference 4.

Experimental lifetime and strength results are presented in table II and are compared with predicted results in figures 8 and 9, respectively. Lifetime data obtained in cyclic-load creep tests are shown as square and triangular symbols in figure 8; data obtained under constant load appear as circular and diamond-shaped symbols. The ordinates of cyclic-load results are in terms of equivalent moment, that is, the moment corresponding to the calculated equivalent stresses. Theoretical lifetimes calculated from equation (10) are shown as curves in the figure. The shallow slope of the curve for beam B suggests high sensitivity of this design to creep load, as mentioned earlier and borne out by the experimental results. The correlation between experimental and calculated lifetime results generally appears to be reasonable in figure 8.

In figure 9 the results of strength tests performed after the beams had been subjected to 20 hours of cyclic loads which did not produce creep are compared with the strength calculated from equation (10) for beams exposed to test temperature for 20 hours without load. The experimental results are represented by square symbols. Experimental and calculated results of the strength tests conducted after 1/2-hour exposure are also given in the figure for comparison. Results indicate that the strength of the beams was not appreciably affected by the cyclic loading. It is pointed out in reference 2 that the relatively low values of creep strain which can be sustained in a built-up structure appear to have no significant effect on structural strength. Results of the present tests indicate that consideration of creep is not of importance at load ranges below two-thirds of the structural strength.

CONCLUDING REMARKS

A method has been developed for calculating the deflection and lifetime of multiweb box beams subjected to creep under varied loads and constant temperature. Deflections are obtained by integrating the classical relationship between beam curvature and strain where the strain is given by a materials creep law. The method also involves the use of the life-fraction rule.

Calculated results were compared with cyclic-load creep-test data obtained at 400° F from eight multiweb box beams which were fabricated

of 2024-T3 aluminum-alloy sheet. Most of the experimental results were in reasonable agreement with calculated results. Similar correlation will probably be found in applications of the computation method to varied-load creep-test data of longer duration. The agreement between calculated and experimental results indicates that the classical relationship between beam curvature and strain can be used in conjunction with a suitable creep law to obtain deflection for beams under more complicated loadings.

Approximate deflection results calculated for buckled beams by application of short-time buckling relationships to the creep problem and by use of equivalent stresses were in agreement with data obtained in the tests. However, further study of the creep mechanism in beams in the buckled condition is necessary to develop a more rigorous theory for such beams.

L
1
4
6
4

It is felt that creep strains of the order experienced by structural components generally do not affect the structural strength. Results of cyclic-load tests during which the loads were lower than those applied in the previous tests indicate that creep effects are not of importance at load ranges below two-thirds of the structural strength.

Langley Research Center,
National Aeronautics and Space Administration,
Langley Air Force Base, Va., March 12, 1962.

APPENDIX

DEFLECTION OF BEAMS IN CREEP

The relationships presented in the text for the deflections of beams subjected to varied-load creep at constant temperature are derived in this appendix. If it is assumed that beam cross sections remain plane during creep, the beam curvature is given in terms of the strains in the tension and compression covers as

$$\frac{d^2y}{dx^2} = \frac{1}{h}(\epsilon_t - \epsilon_c) \tag{A1}$$

Equation (A1) is the fundamental relationship used for the derivation of deflection equations. The final equations are based on materials creep data obtained under constant load at constant temperature; and use is made of the life-fraction rule for the derivation of the varied-load creep relationships.

For the purpose of the analysis, the beam shown in figure 1(a) is treated in two parts as shown in figure 1(b), namely, the inboard region and the outboard region. For the inboard region $x = 0$ at the left-hand support and increases in the direction of the right-hand support; for the outboard region $x = 0$ at the support and increases in the direction of the tip. Deflection y is positive downward in both cases.

Inboard Region

The applied moment is constant over the inboard region of the beam. Thus the stresses and strains in this region are also independent of x, and equation (A1) can be integrated directly with respect to x; the deflection can be determined by application of appropriate boundary conditions.

The boundary conditions are

$$y_{x=0} = y_{x=l_1} = 0 \tag{A2}$$

The slope of the beam is given by

$$\frac{dy}{dx} = \frac{x - \frac{l_1}{2}}{h}(\epsilon_t - \epsilon_c) \tag{A3}$$

and the deflection by

$$y = \frac{x^2 - l_1 x}{2h}(\epsilon_t - \epsilon_c) \tag{A4}$$

When the overall beam follows material creep behavior as described by equation (1) in the text, substitution from equation (1) into equations (A3) and (A4) yields the relations for the slope and deflection of the beam in terms of constant stress as

$$\frac{dy}{dx} = \frac{x - \frac{l_1}{2}}{h}\left[\frac{\sigma_t - \sigma_c}{E} + A\tau^k\left(\sinh\frac{\sigma_t}{\sigma_o} - \sinh\frac{\sigma_c}{\sigma_o}\right)\right] \tag{A5}$$

$$y = \frac{x^2 - l_1 x}{2h}\left[\frac{\sigma_t - \sigma_c}{E} + A\tau^k\left(\sinh\frac{\sigma_t}{\sigma_o} - \sinh\frac{\sigma_c}{\sigma_o}\right)\right] \tag{A6}$$

L
1
4
6
4

The stresses in equations (A5) and (A6) are those which satisfy equations (3) for static equilibrium.

Deflection under varied-load creep is determined by applying directly to equation (A4) the following equation (which is eq. (C4) of ref. 6):

$$\epsilon_i = \frac{\sigma_i}{E} + A\left(\sum_{n=1}^{n=i} \Delta\tau_n \sinh^{1/k}\frac{\sigma_n}{\sigma_o}\right)^k$$

This procedure yields the inboard deflection of the beam after i applications of load as

$$y_i = \frac{x^2 - l_1 x}{2h}\left\{\frac{\sigma_{t,i} - \sigma_{c,i}}{E} + A\left[\left(\sum_{n=1}^{n=i} \Delta\tau_n \sinh^{1/k}\frac{\sigma_{t,n}}{\sigma_o}\right)^k - \left(\sum_{n=1}^{n=i} \Delta\tau_n \sinh^{1/k}\frac{\sigma_{c,n}}{\sigma_o}\right)^k\right]\right\} \tag{A7}$$

Equations (A6) and (A7) do not apply to a beam which has undergone local buckling. When local buckling has occurred, the deflection is determined from equation (A4) by use of isochronous stress-strain and isochronous load-shortening curves. At a given time, strain ϵ_t in

equation (A4) is obtained from the appropriate isochronous stress-strain curve, and ϵ_c is obtained from the corresponding isochronous load-shortening curve. The isochronous load-shortening curve is constructed by application of the post-buckling strain relationship

$$\sqrt{\frac{\epsilon_c}{\epsilon_{cr}}} = \frac{\sigma_e}{\sigma_c} \tag{A8}$$

to the isochronous stress-strain curve. In equation (A8),

$$\epsilon_{cr} = \frac{K\pi^2}{12\left(1 - \mu^2\right)}\left(\frac{t}{b}\right)^2 \tag{A9}$$

It should be noted that application of equation (A8) is restricted to cases in which ϵ_{cr} is of the magnitude usually associated with the elastic region of the material.

The deflection of a buckled beam under varied-load creep is also determined in this manner. However, in this case the isochronous curves are entered at the equivalent stresses computed from equation (9).

Outboard Region

The deflection in the outboard region of the beam is obtained by the solution of equation (A1) with the following boundary conditions:

$$y_{x=0} = 0 \tag{A10}$$

$$\left.\frac{dy}{dx}\right|_{x=0} = \frac{l_1}{2h}\left(\epsilon_t - \epsilon_c\right)$$

in which the slope at $x = 0$ is obtained from equation (A3). As noted previously, in this section $x = 0$ at the support and increases toward the tip.

Considerable simplification is achieved in the derivation of a relationship for y by the assumption that the stresses in the cover plates vary linearly from a maximum at $x = 0$ to zero at $x = l_2$. At high loads this assumption is violated in the vicinity of $x = 0$, but the magnitude of deflections calculated on the basis of this assumption is not expected to be significantly different from results that would be obtained from a more vigorous analysis. Substitution of equation (1)

into equation (A1) and application of the above assumption yield the curvature in the outboard region as

$$\frac{d^2y}{dx^2} = \frac{\sigma_t - \sigma_c}{Eh}\left(1 - \frac{x}{l_2}\right) + \frac{A_T{}^k}{h}\left\{\sinh\left[\frac{\sigma_t}{\sigma_o}\left(1 - \frac{x}{l_2}\right)\right] - \sinh\left[\frac{\sigma_c}{\sigma_o}\left(1 - \frac{x}{l_2}\right)\right]\right\} \tag{A11}$$

and the deflection under constant load as

$$y = \frac{\sigma_t - \sigma_c}{Eh}\left(\frac{l_1 x}{2} + \frac{x^2}{2} - \frac{x^3}{6l_2}\right) + A_T{}^k \frac{l_1 x}{2h}\left(\sinh\frac{\sigma_t}{\sigma_o} - \sinh\frac{\sigma_c}{\sigma_o}\right)$$

$$+ A_T{}^k \frac{l_2{}^2}{h}\left(\left(\frac{\sigma_o}{\sigma_t}\right)^2\left\{\sinh\left[\frac{\sigma_t}{\sigma_o}\left(1 - \frac{x}{l_2}\right)\right] - \sinh\frac{\sigma_t}{\sigma_o}\right\} + \frac{x}{l_2}\frac{\sigma_o}{\sigma_t}\cosh\frac{\sigma_t}{\sigma_o}\right.$$

$$\left. - \left(\frac{\sigma_o}{\sigma_c}\right)^2\left\{\sinh\left[\frac{\sigma_c}{\sigma_o}\left(1 - \frac{x}{l_2}\right)\right] - \sinh\frac{\sigma_c}{\sigma_o}\right\} + \frac{x}{l_2}\frac{\sigma_o}{\sigma_c}\cosh\frac{\sigma_c}{\sigma_o}\right) \tag{A12}$$

where σ_t and σ_c are now the cover stresses at $x = 0$.

In equation (A12) the first term containing hyperbolic sines is the outboard deflection corresponding to the rotation of the tangent at the support and is directly proportional to the inboard rotation. Since this term contains the creep strain explicitly, the life-fraction rule can be applied to obtain the deflection under varied creep. The remaining creep terms in the equation are not explicit functions of strain, and the life-fraction rule does not apply. This problem may be avoided by introduction of the life-fraction rule into equation (A11) for beam curvature and the use of numerical integration procedures. In the present study, the total deflection under varied loads was obtained in an approximate manner by treating the last term in equation (A12) similarly to the first creep-deflection term. The error introduced into the calculated results is probably small, because the last term in equation (A12) contributes less than 10 percent of the beam deflection at the tip. The deflection of the outboard region of the beam then becomes

$$y_i = \frac{\sigma_{t,i} - \sigma_{c,i}}{Eh}\left(\frac{l_1 x}{2} + \frac{x^2}{2} - \frac{x^3}{6l_2}\right) + A\,\frac{l_1 x}{2h}\left[\left(\sum_{n=1}^{n=i} \Delta\tau_n \sinh^{1/k} \frac{\sigma_{t,n}}{\sigma_o}\right)^k\right.$$

$$\left. - \left(\sum_{n=1}^{n=i} \Delta\tau_n \sinh^{1/k} \frac{\sigma_{c,n}}{\sigma_o}\right)^k\right] + \frac{Al_2^2}{h}\left[\sum_{n=1}^{n=i} \Delta\tau_n \left(\left(\frac{\sigma_o}{\sigma_{t,n}}\right)^2 \left\{\sinh\left[\frac{\sigma_{t,n}}{\sigma_o}\left(1 - \frac{x}{l_2}\right)\right]\right.\right.$$

$$\left.\left. - \sinh \frac{\sigma_{t,n}}{\sigma_o}\right\} + \frac{x}{l_2}\frac{\sigma_o}{\sigma_{t,n}} \cosh \frac{\sigma_{t,n}}{\sigma_o}\right)^{1/k}\Bigg]^k$$

$$- \frac{Al_2^2}{l}\left[\sum_{n=1}^{n=i} \Delta\tau_n \left(\left(\frac{\sigma_o}{\sigma_{c,n}}\right)^2 \left\{\sinh\left[\frac{\sigma_{c,n}}{\sigma_o}\left(1 - \frac{x}{l_2}\right)\right] - \sinh \frac{\sigma_{c,n}}{\sigma_o}\right\}\right.\right.$$

$$\left.\left. + \frac{x}{l_2}\frac{\sigma_o}{\sigma_{c,n}} \cosh \frac{\sigma_{c,n}}{\sigma_o}\right)^{1/k}\right]^k \qquad \text{(A13)}$$

Equations (A12) and (A13) have been developed for a beam in which the compression cover remains unbuckled. The effect of buckling on the deflection of the outboard region of the beam is mainly in the first creep-deflection term which represents the deflection due to rotation at the support. This can be accounted for by substitution of the following expression for this term in equation (A12):

$$\frac{l_1 x}{2h}(\epsilon_t - \epsilon_c)_{creep}$$

where ϵ_t and ϵ_c denote the creep strains in the inboard covers and are evaluated from isochronous stress-strain and load-shortening curves, respectively, as described previously in the appendix. Under varied-load creep the outboard deflection of a buckled beam is determined by the same procedure, the isochronous curves being used in conjunction with equivalent stresses calculated from equation (9) in the text.

REFERENCES

1. Mathauser, Eldon E.: Investigation of Static Strength and Creep Behavior of an Aluminum-Alloy Multiweb Box Beam at Elevated Temperatures. NACA TN 3310, 1954.

2. Heldenfels, Richard R., and Mathauser, Eldon E.: A Summary of NACA Research on the Strength and Creep of Aircraft Structures at Elevated Temperatures. NACA RM L56D06, 1956.

3. Mathauser, Eldon E., and Deveikis, William D.: Investigation of the Compressive Strength and Creep Lifetime of 2024-T3 Aluminum-Alloy Plates at Elevated Temperatures. NACA Rep. 1308, 1957. (Supersedes NACA TN 3552.)

4. Mathauser, Eldon E., Berkovits, Avraham, and Stein, Bland A.: Recent Research on the Creep of Airframe Components. NACA TN 4014, 1957.

5. Mordfin, Leonard: Analytical Study of Creep Deflection of Structural Beams. NASA TN D-661, 1960.

6. Berkovits, Avraham: Investigation of Three Analytical Hypotheses for Determining Material Creep Behavior Under Varied Loads, With an Application to 2024-T3 Aluminum-Alloy Sheet in Tension at 400° F. NASA TN D-799, 1961.

7. Shanley, F. R.: Weight-Strength Analysis of Aircraft Structures. McGraw-Hill Book Co., Inc., 1952.

8. Zender, George W., and Hall, John B., Jr.: Combinations of Shear, Compressive Thermal, and Compressive Load Stresses for the Onset of Permanent Buckles in Plates. NASA TN D-384, 1960.

TABLE I.- DIMENSIONS OF 2024-T3 ALUMINUM-ALLOY MULTIWEB BOX BEAMS

(a) Nominal $\frac{b}{t} = 25$; $l_1 = l_2 = l$

[b = 3.12 in.; flange width = 0.65 in.; web bend radius = $\frac{3}{16}$ in.; rivet offset = 0.41 in.; rivet diameter = $\frac{5}{32}$ in.; rivet pitch = $\frac{5}{8}$ in.]

Beam	Cover plates			Web thickness, in.	h, in.	l, in.	Total length, in.
	Width, in.	Compression cover thickness, in.	Tension cover thickness, in.				
A1	10.01	0.127	0.162	0.066	3.37	31.0	96.0
A2	10.02	.122	.160	.066	3.38	31.0	96.0
A3	10.00	.126	.157	.065	3.33	31.0	96.0
A4	10.00	.125	.159	.065	3.36	31.0	96.0
A5	10.01	.123	.161	.065	3.35	31.0	96.0
A6	10.00	.122	.160	.066	3.35	31.0	96.0
A7	10.00	.124	.159	.064	3.34	31.0	96.1
A8	10.15	.123	.162	.066	3.35	31.0	96.0
A9	10.02	.122	.163	.066	3.38	31.0	96.0
A10	10.00	.126	.159	.064	3.36	31.0	96.0

(b) Nominal $\frac{b}{t} = 40$; $l_1 = l_2 = l$

[b = 3.24 in.; flange width = 0.52 in.; web bend radius = $\frac{5}{32}$ in.; rivet offset = 0.33 in.; rivet diameter = $\frac{1}{8}$ in. rivet pitch = $\frac{1}{2}$ in.]

Beam	Cover plates			Web thickness, in.	h, in.	l, in.	Total length, in.
	Width, in.	Compression cover thickness, in.	Tension cover thickness, in.				
B1	10.24	0.080	0.079	0.059	3.37	31.0	96.0
B2	10.25	.079	.078	.060	3.36	31.0	96.0
B3	10.25	.079	.078	.052	3.38	31.0	96.0
B4	10.25	.080	.079	.059	3.40	31.0	96.0
B5	10.25	.078	.079	.052	3.43	31.0	96.0
B6	10.25	.078	.078	.052	3.43	31.0	96.0
B7	10.25	.079	.079	.052	3.42	31.0	96.0
B8	10.25	.078	.078	.053	3.40	31.0	96.1
B9	10.25	.078	.078	.053	3.42	31.0	96.1

TABLE II.- TEST CONDITIONS AND FAILURE DATA OBTAINED

(a) Strength tests

Beam	Type of test	Temperature, °F	M_{ult}, in-kips
A1	Static strength	400	174.4
A8	(a)	400	211.6
A9	(b)	400	208.0
A10	(b)	500	122.8
B1	Static strength	400	105.9
B2	Static strength	400	100.8
B8	(a)	400	102.5
B9	(b)	400	92.1

[a]20 hours under cyclic loads as given by curve C of figure 4, followed by strength test.

[b]20 hours under cyclic loads as given by curve B of figure 4, followed by strength test.

(b) Creep tests

[400° F test temperature]

Beam	Type of test	Loads applied, in-kips			Lifetime, hr
		M_1	M_2	M_3	
A2	Constant load	161.2	-----	-----	6.1
A3	Cyclic load	121.0	151.2	165.8	10.0
A4	Cyclic load	105.3	139.3	161.2	29.5
A5	Cyclic load	161.2	139.3	105.3	19.1
A6	Cyclic load	161.2	139.3	105.3	12.6
A7	Cyclic load	161.2	139.3	105.3	18.7
B3	Constant load	91.5	-----	-----	.2
B4	Constant load	77.5	-----	-----	81.9
B5	Cyclic load	78.7	82.9	84.6	.8
B6	Cyclic load	77.5	81.6	83.1	9.5
B7	Cyclic load	83.1	81.6	77.5	9.2

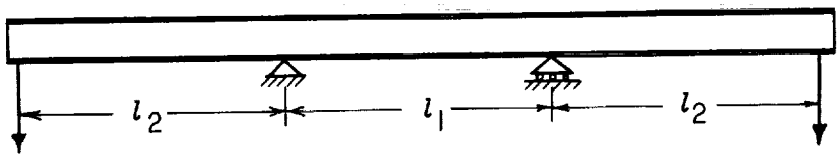

(a) Support locations and points of application of loads.

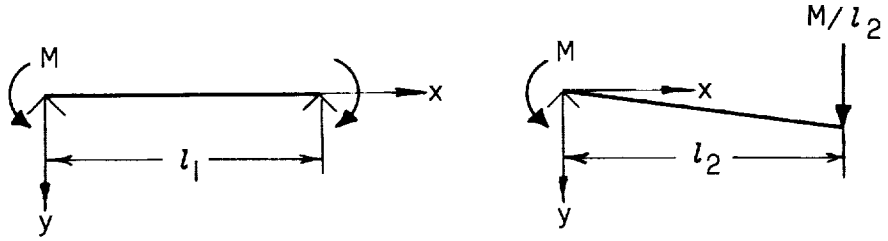

(b) Coordinate systems used in analyses.

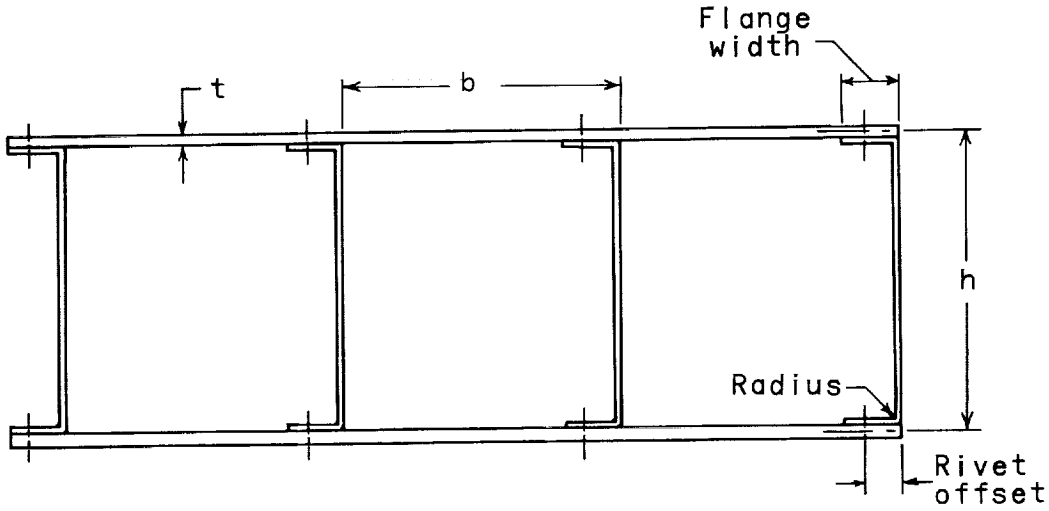

(c) Beam cross section.

Figure 1.- Schematic representation of beam investigated.

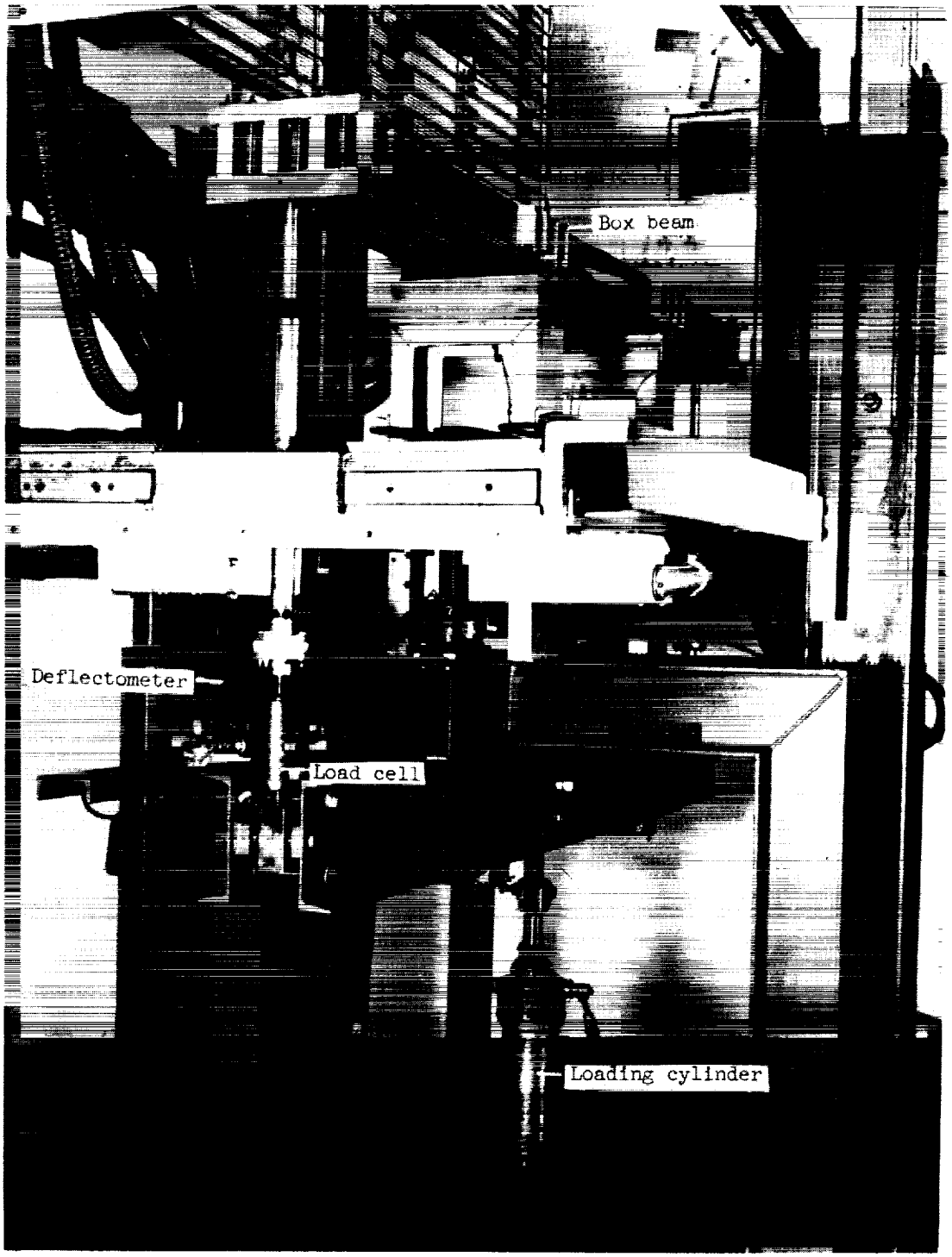

L-1464

Figure 2.- View of multiweb box beam in furnace. L-59-4276.1

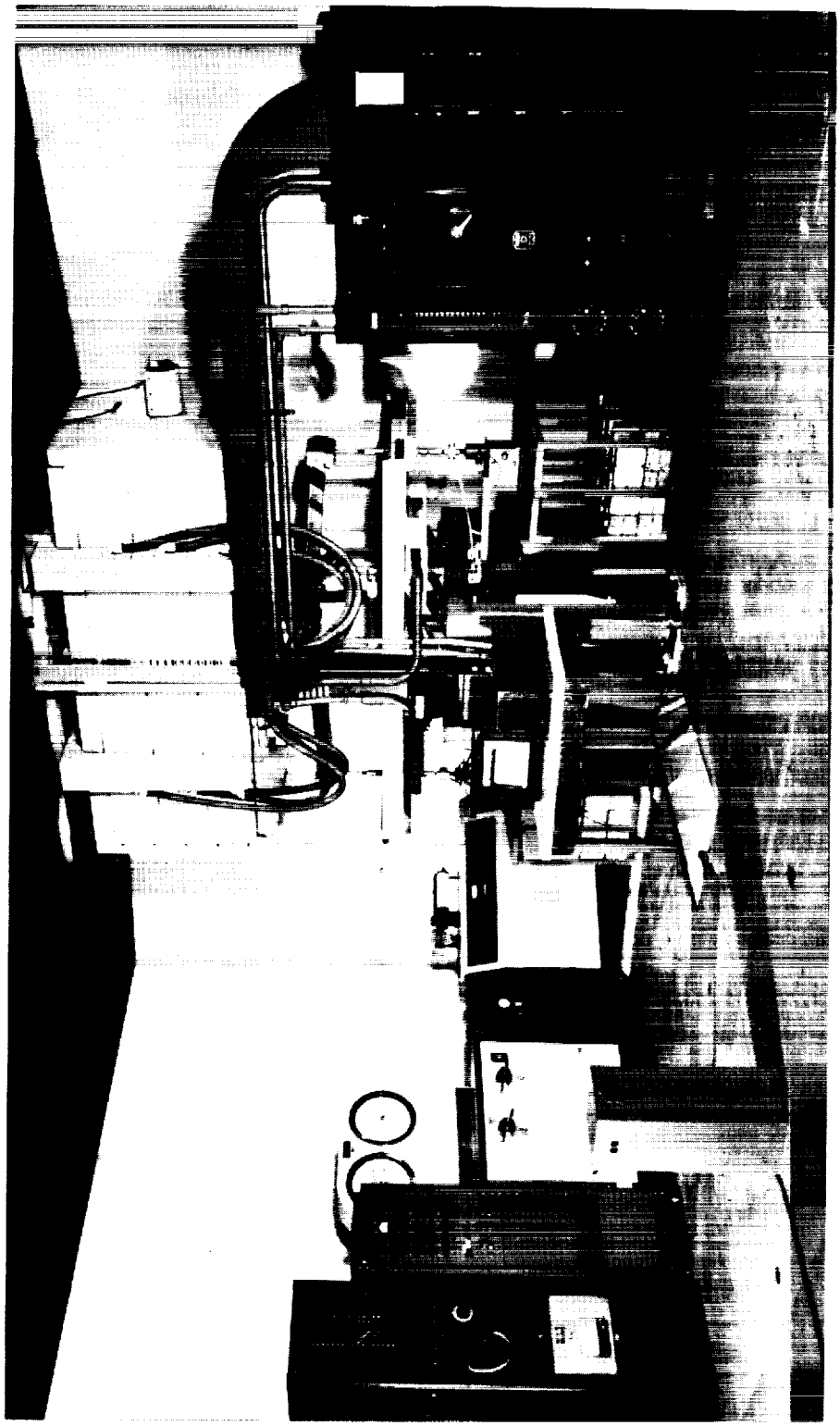

L-58-1026a

Figure 3.- Test equipment.

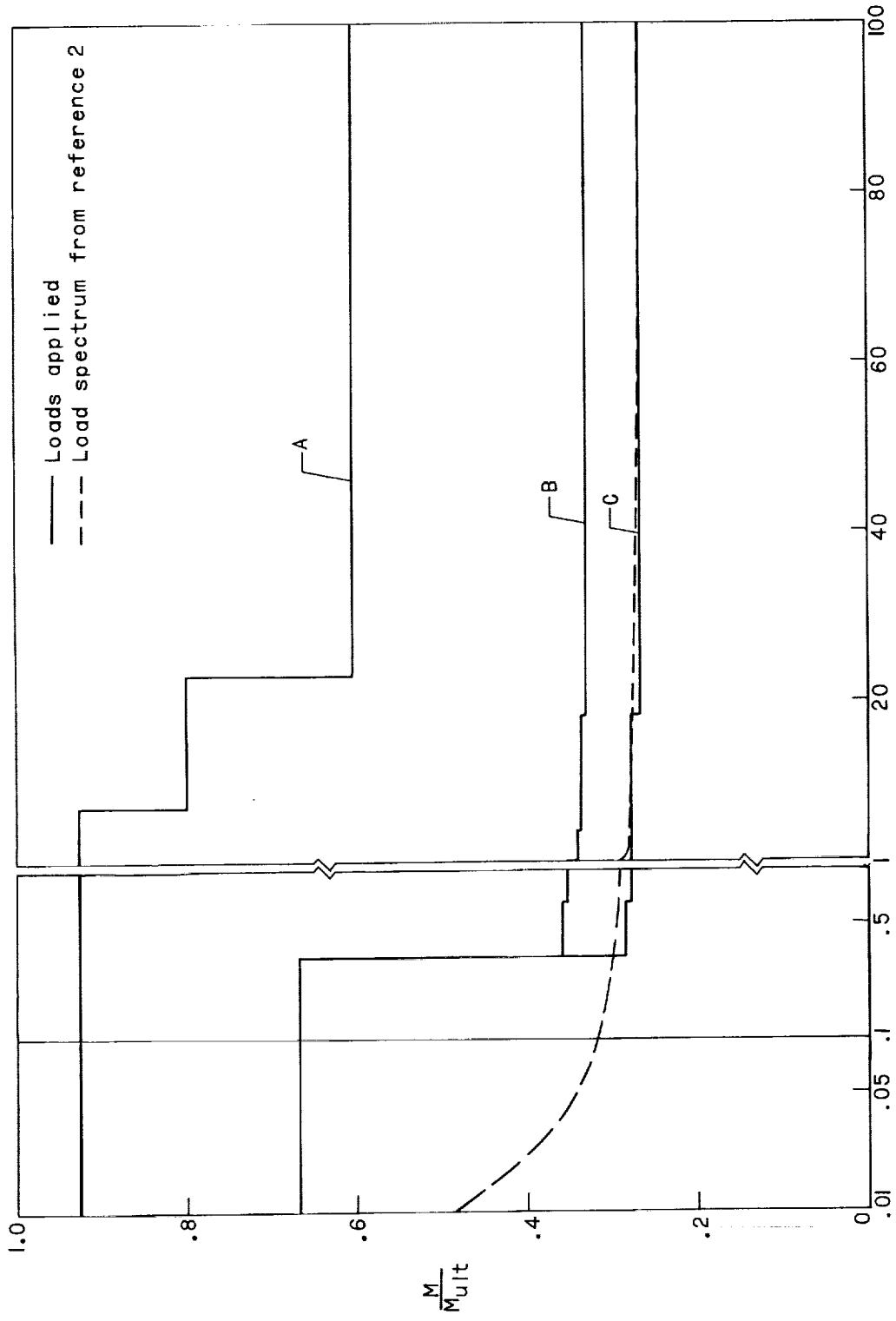

Figure 4.- Load-time distributions applied during cyclic-load creep tests.

L-1464

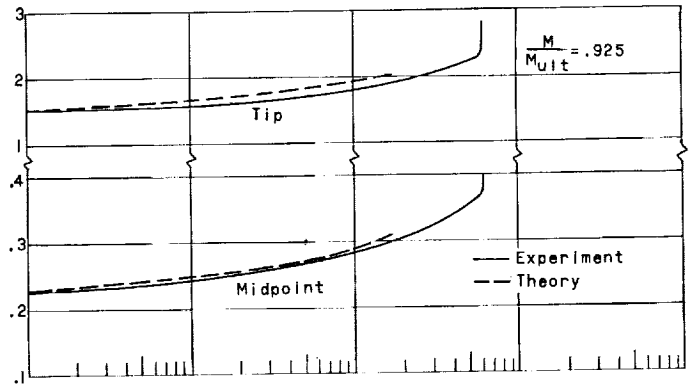

(a) Beam A2.

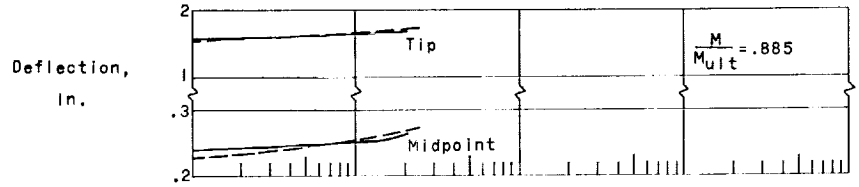

(b) Beam B3.

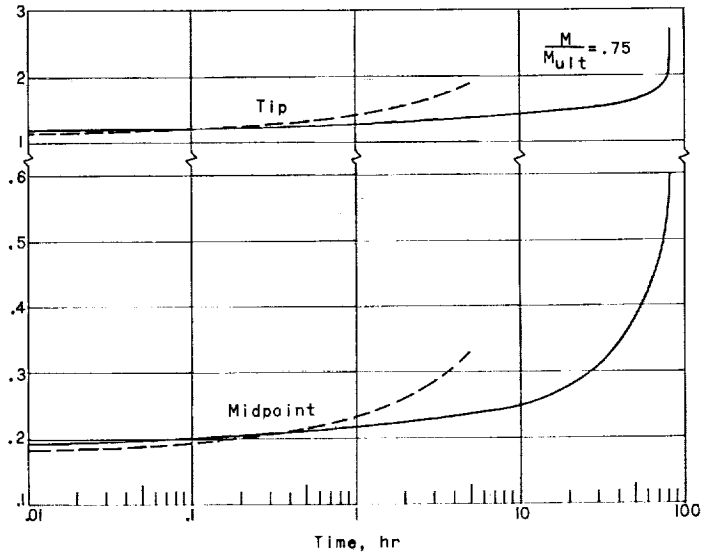

(c) Beam B4.

Figure 5.- Comparison between calculated and experimental deflections of 2024-T3 aluminum-alloy multiweb box beams under constant load at 400° F.

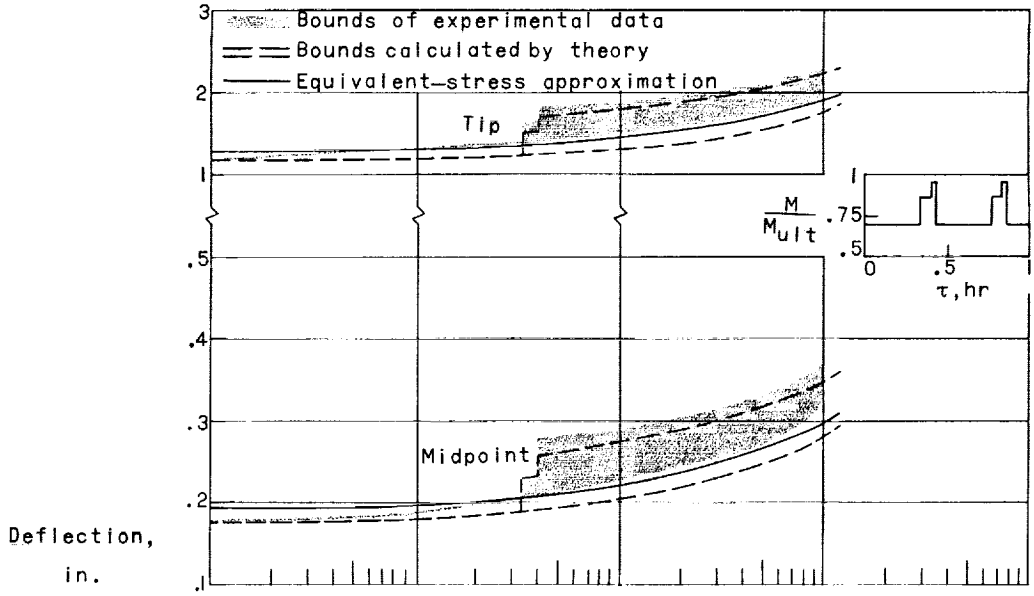

(a) Beam A3.

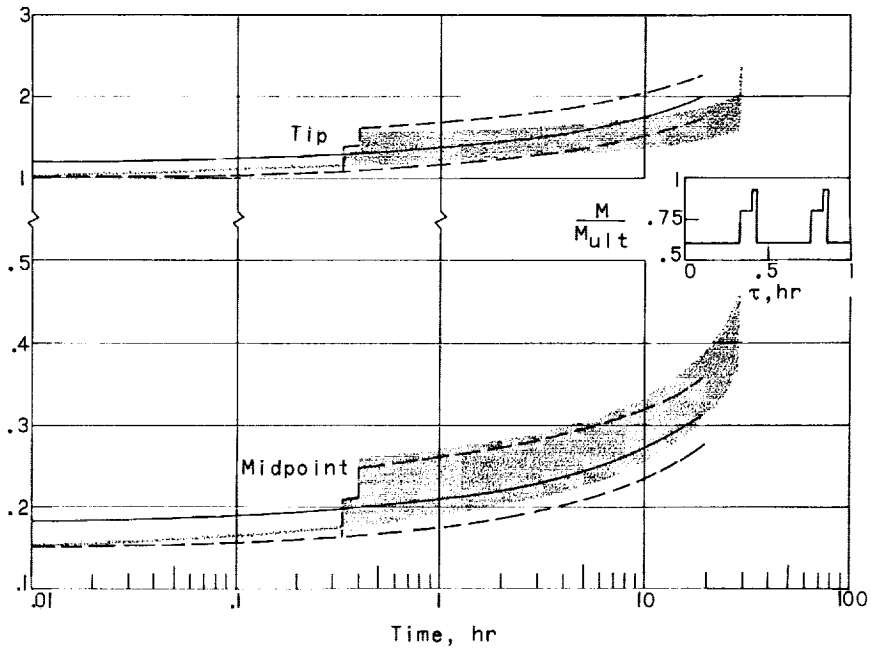

(b) Beam A4.

Figure 6.- Comparison between calculated and experimental deflections of 2024-T3 aluminum-alloy multiweb box beams under cyclic loads at 400° F.

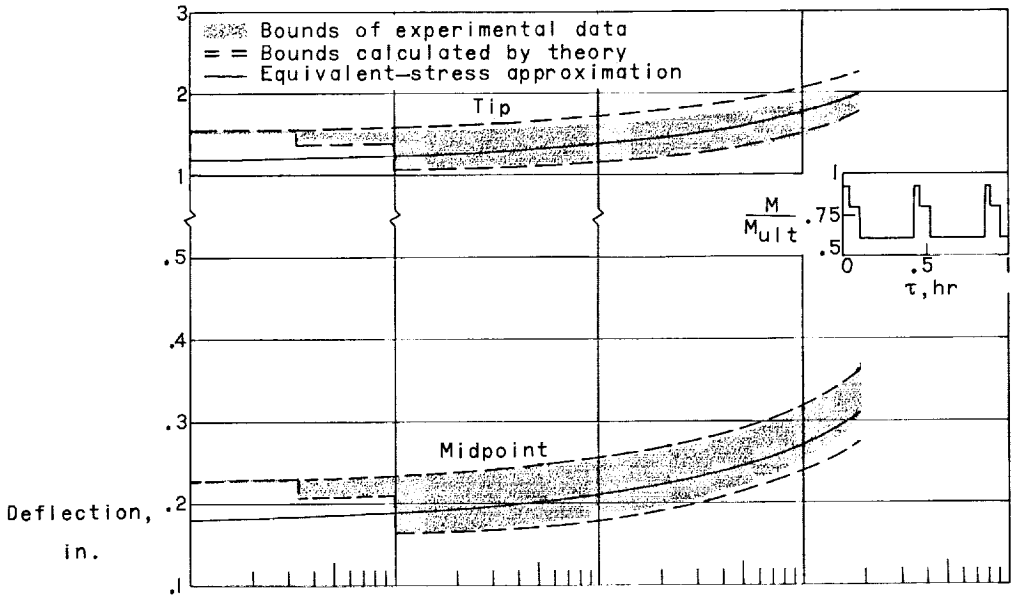

(c) Beam A5.

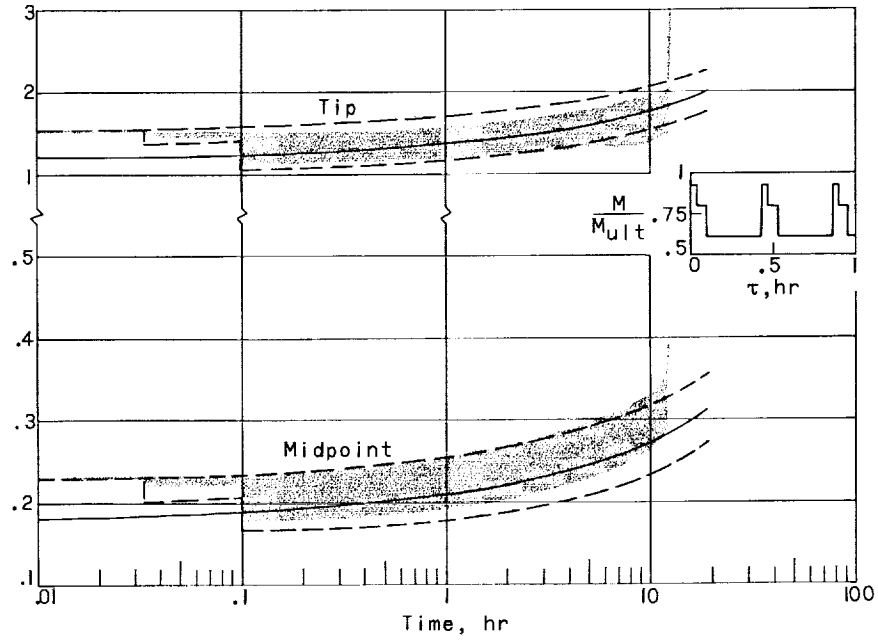

(d) Beam A6.

Figure 6.- Continued.

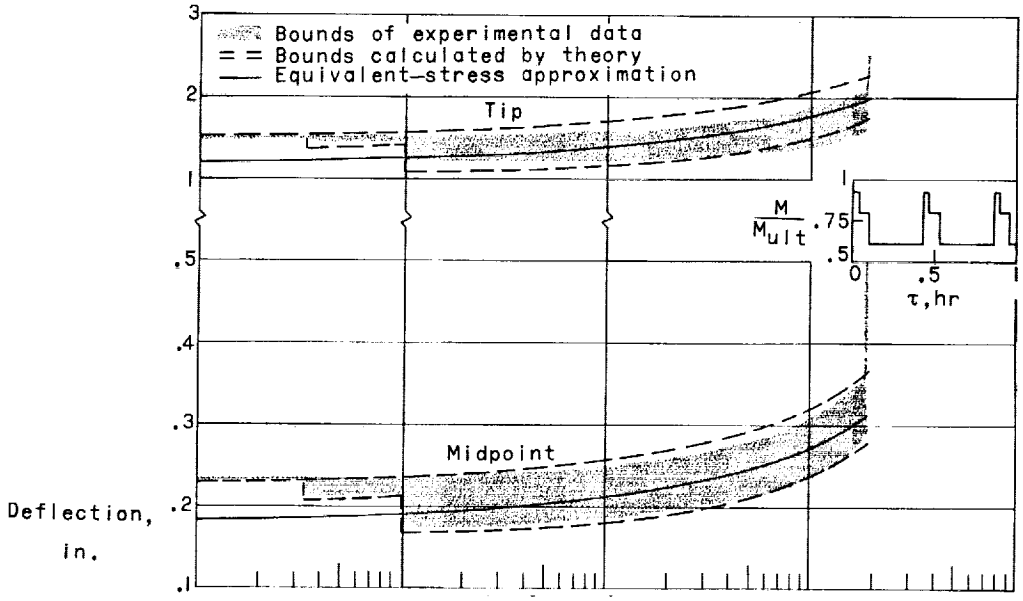

(e) Beam A7.

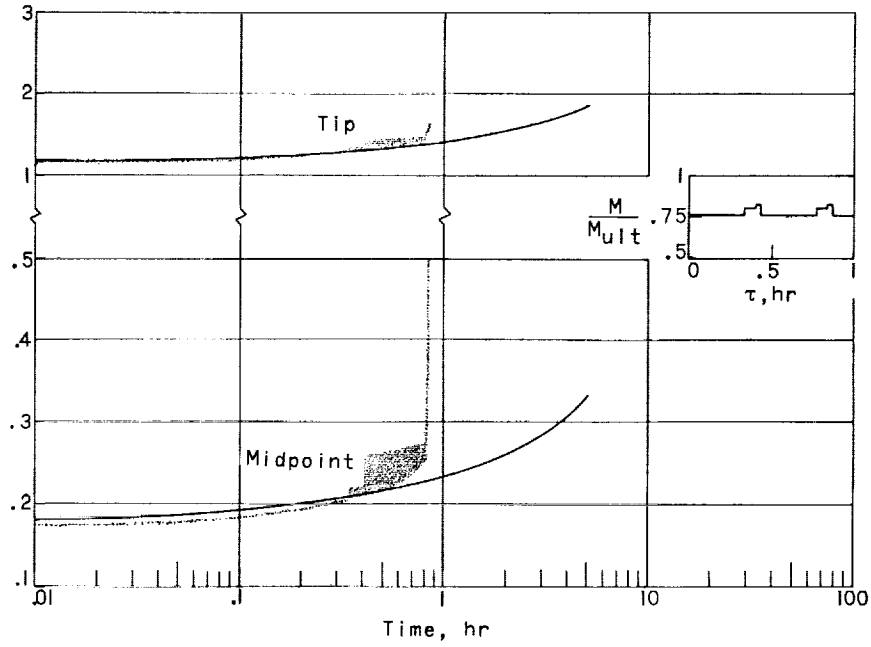

(f) Beam B5.

Figure 6.- Continued.

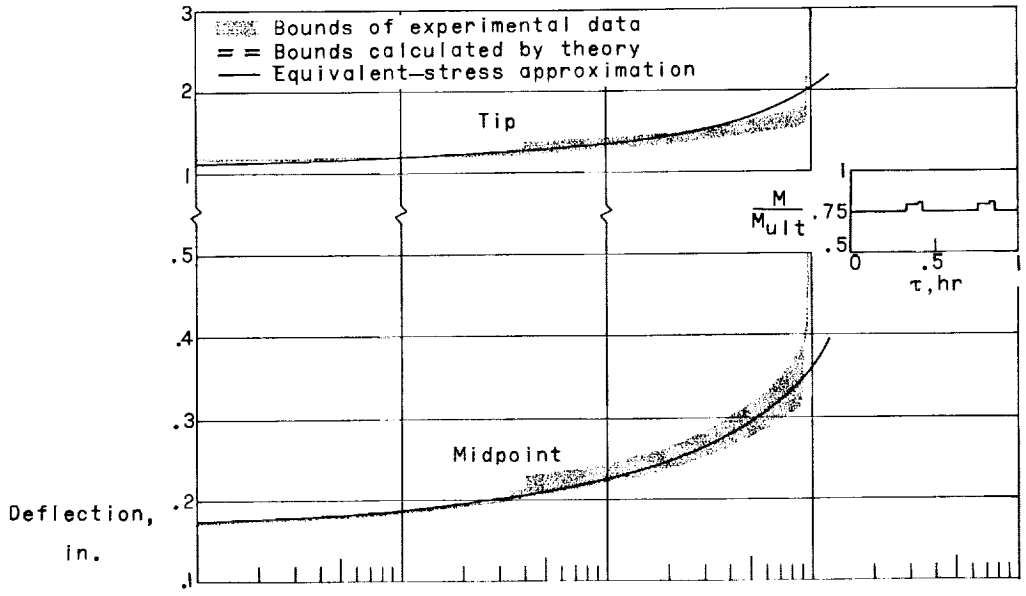

(g) Beam B6.

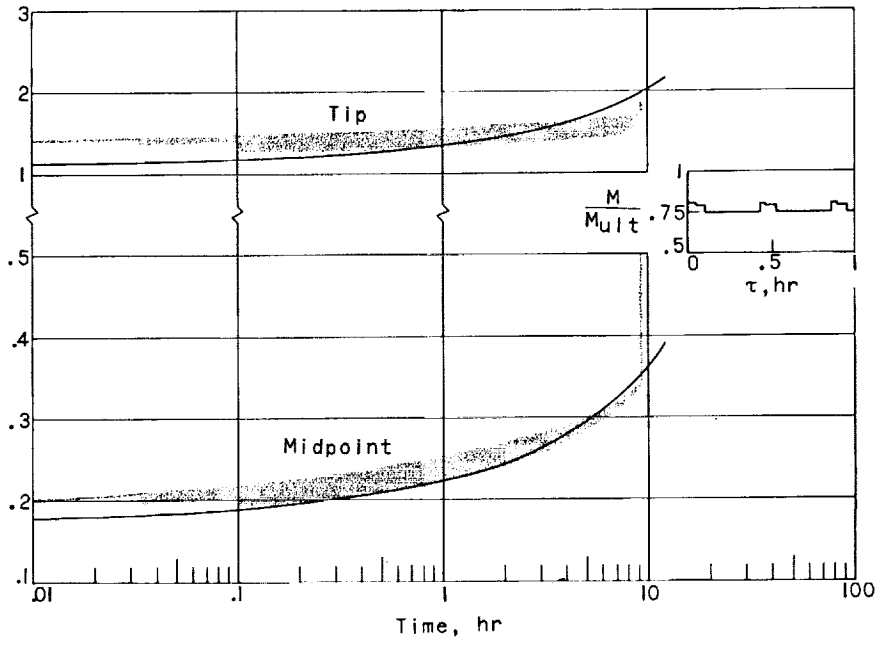

(h) Beam B7.

Figure 6.- Concluded.

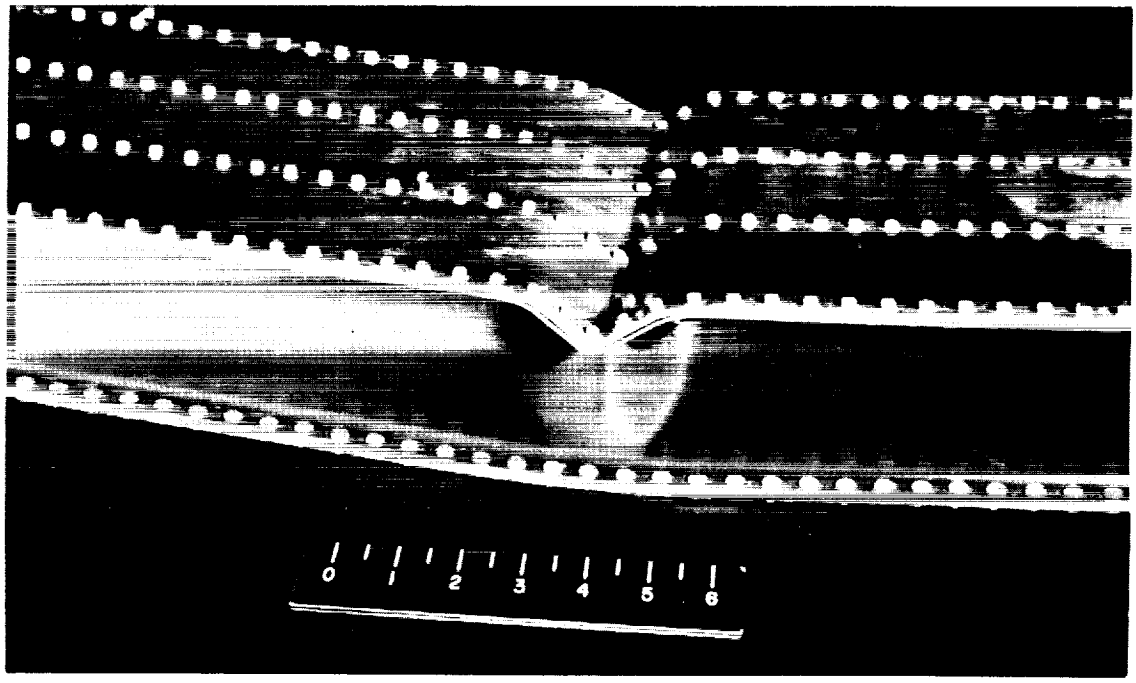

(a) Beam A7. L-59-4281

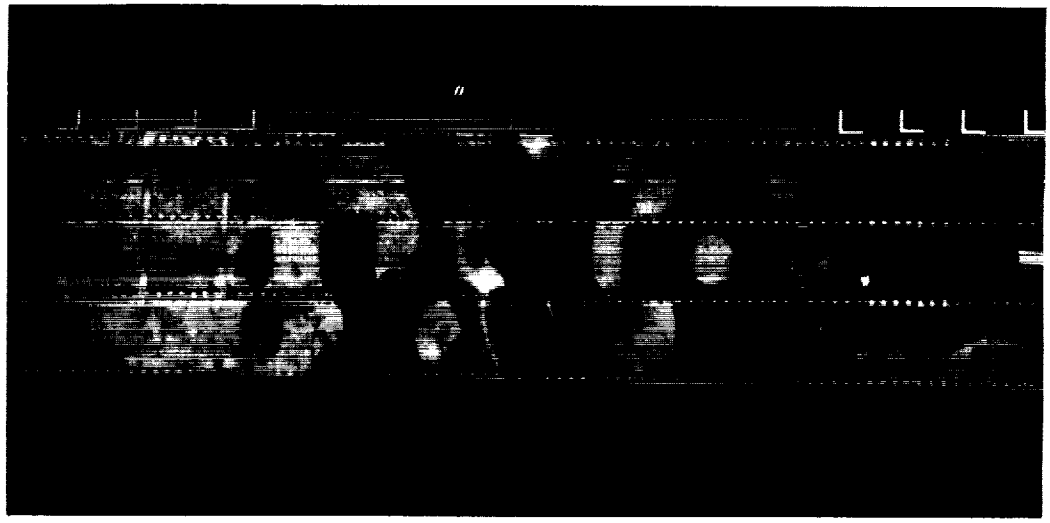

(b) Beam B4. L-59-4285

Figure 7.- Typical failures of 2024-T3 aluminum-alloy multiweb box beams.

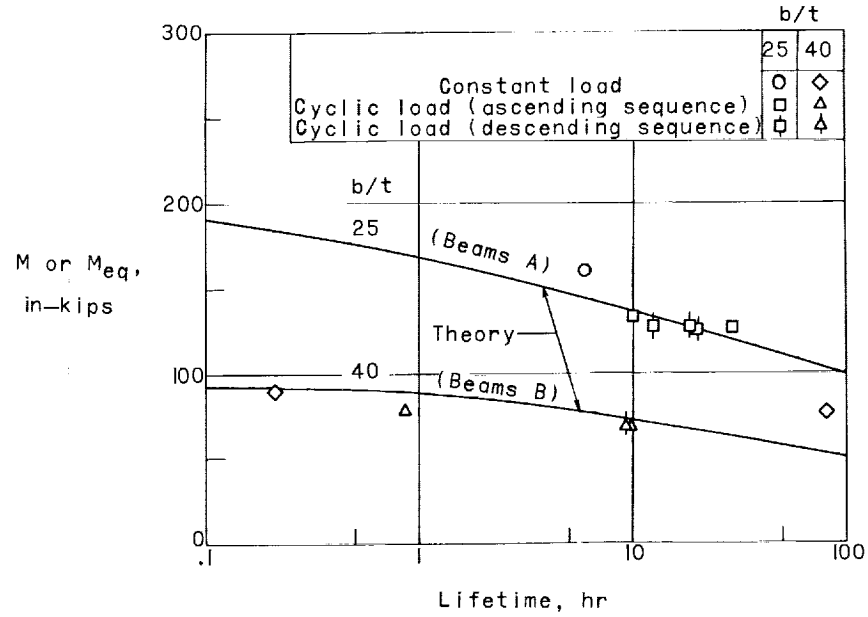

Figure 8.- Comparison between predicted and experimental creep lifetimes under cyclic and constant loads for 2024-T3 aluminum-alloy multiweb box beams at 400° F.

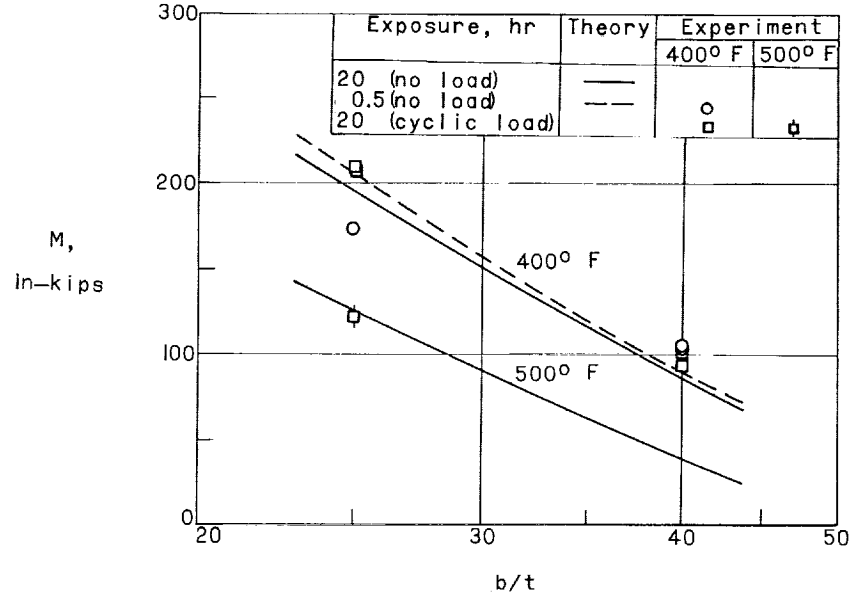

Figure 9.- Comparison between predicted and experimental strength of 2024-T3 aluminum-alloy multiweb box beams after exposure to cyclic creep loads.

NASA-Langley, 1962 L-1464

L-1464

NASA TN D-1265
National Aeronautics and Space Administration.
DETERMINATION OF THE CREEP DEFLECTION AND LIFETIME OF ALUMINUM-ALLOY MULTIWEB BOX BEAMS SUBJECTED TO VARIED LOADS AT CONSTANT TEMPERATURE. Avraham Berkovits. June 1962. 33p. OTS price, $1.00.
(NASA TECHNICAL NOTE D-1265)

A method was developed for computing the deflection and lifetime of multiweb box beams subjected to creep under varied loads at constant temperatures. The method of analysis is based on the life-fraction rule and materials creep data obtained from constant-load and constant-temperature tensile creep tests. Calculated deflection and lifetime results are compared with corresponding test data from multiweb box beams fabricated from 2024-T3 aluminum-alloy sheet and tested at 400° F under cyclic creep loads. An equivalent-stress concept is utilized in a portion of this study to reduce the varied-load creep problem to creep under constant stress.

I. Berkovits, Avraham
II. NASA TN D-1265

(Initial NASA distribution: 51, Stresses and loads.)

NASA

NASA TN D-1265
National Aeronautics and Space Administration.
DETERMINATION OF THE CREEP DEFLECTION AND LIFETIME OF ALUMINUM-ALLOY MULTIWEB BOX BEAMS SUBJECTED TO VARIED LOADS AT CONSTANT TEMPERATURE. Avraham Berkovits. June 1962. 33p. OTS price, $1.00.
(NASA TECHNICAL NOTE D-1265)

A method was developed for computing the deflection and lifetime of multiweb box beams subjected to creep under varied loads at constant temperatures. The method of analysis is based on the life-fraction rule and materials creep data obtained from constant-load and constant-temperature tensile creep tests. Calculated deflection and lifetime results are compared with corresponding test data from multiweb box beams fabricated from 2024-T3 aluminum-alloy sheet and tested at 400° F under cyclic creep loads. An equivalent-stress concept is utilized in a portion of this study to reduce the varied-load creep problem to creep under constant stress.

I. Berkovits, Avraham
II. NASA TN D-1265

(Initial NASA distribution: 51, Stresses and loads.)

NASA

NASA TN D-1265
National Aeronautics and Space Administration.
DETERMINATION OF THE CREEP DEFLECTION AND LIFETIME OF ALUMINUM-ALLOY MULTIWEB BOX BEAMS SUBJECTED TO VARIED LOADS AT CONSTANT TEMPERATURE. Avraham Berkovits. June 1962. 33p. OTS price, $1.00.
(NASA TECHNICAL NOTE D-1265)

A method was developed for computing the deflection and lifetime of multiweb box beams subjected to creep under varied loads at constant temperatures. The method of analysis is based on the life-fraction rule and materials creep data obtained from constant-load and constant-temperature tensile creep tests. Calculated deflection and lifetime results are compared with corresponding test data from multiweb box beams fabricated from 2024-T3 aluminum-alloy sheet and tested at 400° F under cyclic creep loads. An equivalent-stress concept is utilized in a portion of this study to reduce the varied-load creep problem to creep under constant stress.

I. Berkovits, Avraham
II. NASA TN D-1265

(Initial NASA distribution: 51, Stresses and loads.)

NASA

NASA TN D-1265
National Aeronautics and Space Administration.
DETERMINATION OF THE CREEP DEFLECTION AND LIFETIME OF ALUMINUM-ALLOY MULTIWEB BOX BEAMS SUBJECTED TO VARIED LOADS AT CONSTANT TEMPERATURE. Avraham Berkovits. June 1962. 33p. OTS price, $1.00.
(NASA TECHNICAL NOTE D-1265)

A method was developed for computing the deflection and lifetime of multiweb box beams subjected to creep under varied loads at constant temperatures. The method of analysis is based on the life-fraction rule and materials creep data obtained from constant-load and constant-temperature tensile creep tests. Calculated deflection and lifetime results are compared with corresponding test data from multiweb box beams fabricated from 2024-T3 aluminum-alloy sheet and tested at 400° F under cyclic creep loads. An equivalent-stress concept is utilized in a portion of this study to reduce the varied-load creep problem to creep under constant stress.

I. Berkovits, Avraham
II. NASA TN D-1265

(Initial NASA distribution: 51, Stresses and loads.)

NASA